4. H.-D. Chen, J.-S. Chen, and Y.-T. Cheng, Modified inverted-L monopole antenna for 2.4/5 GHz dual band operation, Electron Lett 39 (2003).
5. Z. Zhang, M.F. Iskander, J.-C. Langer, and J. Mathew, Dual band WLAN dipole antenna using an internal matching circuit, IEEE Trans Antennas Propag 53 (2005), 1813–1818.
6. M.N. Suma, R.K. Raj, M. Joseph, P.C. Bybi, and P. Mohanan, A compact dual band branched monopole antenna for DCS/2.4GHz WLAN applications, IEEE Microw Wireless Comp Lett 16 (2006), 275–277.
7. R.K. Raj, M. Joseph, C.K. Anandan, K. Vasudevan, and P. Mohanan, A new compact microstrip-fed dual-band coplanar antenna for WLAN applications, IEEE Trans Antennas Propag 54 (2006), 3755–3762.
8. Y.C. Lin and K.J. Hung, Design of dual-band slot antenna with double T-match stubs, Electron Lett 42 (2006), 438–439.
9. J.Y. Jan and J.W. Su, Bandwidth enhancement of a printed wide-slot antenna with a rotated slot, IEEE Trans Antennas Propag 53 (2005), 2111–2114.
10. Y.F. Liu, K.L. Lau, Q. Xue, and C.H. Chen, Experimental studies of printed wide-slot antenna for wide-band applications, IEEE Antennas Wireless Propag Lett 3 (2004), 273–275.
11. C.-Y. Pan, T.-S. Horng, W.-S. Chen, and C.-H. Huang, Dual wideband printed monopole antenna for WLAN/WiMax applications, IEEE Antennas Wireless Propag Lett 6 (2007), 149–151.
12. W.C Liu and H.J Liu, Compact tri-band slotted monopole antenna with asymmetrical CPW grounds, Electron Lett 42 (2006), 840–842.
13. W.-S Chen and K.-Y Ku, Band-rejected design of printed open slot antenna for WLAN/WiMAX operation, IEEE Trans Antennas Propag 56 (2008), 1163–1169.

MULTIBAND ANTENNA USING +1,−1, AND 0 RESONANT MODE OF DGS DUAL COMPOSITE RIGHT/LEFT HANDED TRANSMISSION LINE

Young-Ho Ryu,[1] Jae-Hyun Park,[2] Jeong-Hae Lee,[2] and Heung-Sik Tae[1]
[1] School of Electrical, Engineering and Computer Science, Kyungpook National University, Korea
[2] Department of Electrical Engineering, Hongik University, Korea; Corresponding author: jeonglee@hongik.ac.kr

Received 7 January 2009

ABSTRACT: *The multiband antenna using defected ground structure (DGS) dual composite right/left handed transmission line (D-CRLH TL) is proposed. The D-CRLH TL resonator can provide a multiband using positive, zero, and negative modes without the different length resonators because the D-CRLH TL has inherent three bands in half periodicity. To design and analyze the proposed antenna, the circuit simulation of the two stage DGS D-CRLH resonator is executed by the equivalent circuit and the results are compared with those of full wave simulation and experiment. The results show that the presented antenna has such a reasonable radiation characteristics of efficiency, bandwidth, and size that it is suitable for compact multiband antenna. In addition, a theoretically unexpected radiation mode, which is generated by the DGS, is observed in the stop band. This additional mode could be utilized for the multi-band antenna.* © 2009 Wiley Periodicals, Inc. Microwave Opt Technol Lett 51: 2485–2488, 2009; Published online in Wiley InterScience (www.interscience.wiley.com). DOI 10.1002/mop.24649

Key words: *metamaterial; D-CRLH transmission line; multiband antenna; defected ground structure*

1. INTRODUCTION

Multiband antennas with good radiation characteristics have been developed widely and rapidly for Modern Wireless communications such as wireless local area network (WLAN) and personal communication transceiver systems. Many multiband antennas such as inverted-F antennas (IFAs) and planar inverted-F antennas (PIFAs) [1–4] and fractal antennas [5, 6] have been successfully designed as a compact high-performance multiband planar antenna. These antennas based on conventional transmission lines (TLs) with the single branch of dispersion curve use multi separate resonant paths of different length of resonators operated at half- or quarter- wavelength modes to obtain the multiple resonances. On the other hand, metamaterial TLs have inherent multiband property, so that they can be utilized as a multiband antenna using positive, zero, and negative modes without any different length resonators [7, 8]. However, these antennas are not suitable for multiband antennas since they have poor radiation properties such as poor radiation efficiency at the negative modes.

In this article, a resonant antenna using dual composite left/right handed transmission lines (D- CRLH TLs) as a multi-band application is proposed. Recently, the novel concepts of dual composite left/right handed transmission lines (D-CRLH TLs) are introduced [9, 10]. D-CRLH TL has a dual concept of CRLH TL and its planar type of transmission line using a defected ground structure (DGS) has been reported [11]. However, it has three branches of dispersion curves within half periodicity since it has an additional right handed branch due to an inherent series inductance and shunt capacitance [11]. Thus, this planar D-CRLH TL has an advantage of multiband application in comparison with CRLH TLs and conventional TLs. The DGS D-CRLH TL resonator consists of DGS and stub with rectangular patch [11]. To analyze the resonant modes of the resonator, the theoretical analysis and circuit simulation are executed using the equivalent circuit. The multiband antenna is designed based on the aforementioned results. To confirm the properties of the multiband antenna such as radiation pattern, fractional bandwidth, gain, and efficiency, the antenna is implemented and its characteristics are measured. The compared results of theory, simulation, and experiment will be presented. In addition, the effects of radiation loss of the DGS will also be analyzed.

2. DEFECTED GROUND STRUCTURE DUAL-CRLH TRANSMISSION LINE

2.1. Unit Cell Structure and Equivalent Circuit

Figure 1 shows the top and bottom view of the unit cell of DGS D-CRLH TL [11]. The unit cell consists of stub with rectangular patch on signal line and DGS with inter-digital gap. The DGS is equivalently modeled as a parallel LC resonant circuit connected in series on host transmission. The stub with rectangular patch is represented by a series LC resonance tank connected in shunt between the signal and ground line, as shown in Figure 2. Since these two structures have band-stop characteristic with negative permeability and permittivity, respectively, the DGS D-CRLH TL can be constructed with combination of two structures.

In order to obtain the balanced condition of DGS D-CRLH TL [11, 12], using the circuit and full wave simulation, the circuit parameters of unit cell are set to be L_d = 6.42 nH, C_d = 0.41 pF, L_s = 12.55 nH, C_p = 0.21 pF, L_t = 4.77 nH, and C_t = 0.16 pF, respectively. The resulting dimensions of structure of DGS D-CRLH TL are shown in Figure 1 to have the above values of circuit parameters.

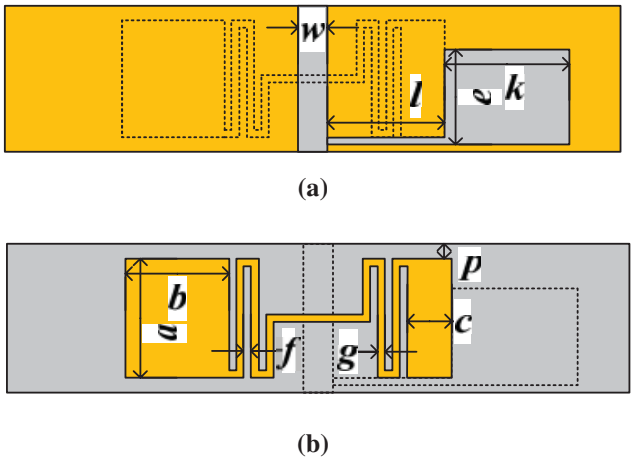

Figure 1 Structure of DGS D-CRLH TL (unit cell). (a) Top view, (b) Bottom view ($a = b = 5$ mm, $c = 2.5$ mm, $e = 3$ mm, $f = 0.2$ mm, $g = 0.2$ mm, $k = 5.7$ mm, $l = 3.9$ mm, $w = 2$ mm, $p = 0.5$ mm). [Color figure can be viewed in the online issue, which is available at www.interscience.wiley.com]

2.2. Theory

The series impedance (Z) and shunt admittance (Y) in Figure 2 can be obtained as [9],

$$Z(\omega) = j\omega L_i \frac{\omega^2 - \omega_{Z0}^2}{\omega^2 - \omega_{Z\infty}^2} \tag{1}$$

$$Y(\omega) = j\omega C_l \frac{\omega^2 - \omega_{Y0}^2}{\omega^2 - \omega_{Y\infty}^2}$$

where $\omega_{Z\infty} = \frac{1}{\sqrt{C_d L_d}}$, $\omega_{Y\infty} = \frac{1}{\sqrt{C_p L_s}}$, $\omega_{Z0} = \sqrt{\frac{L_t + L_d}{C_d L_d L_t}}$, and $\omega_{Y0} = \sqrt{\frac{C_t + C_p}{C_p L_s C_t}}$.

By applying the periodic boundary condition related with Bloch-Floquet theorem to the equivalent circuit of the unit cell, the dispersion relation is obtained as,

$$\beta(\omega) = \frac{1}{d}\cos^{-1}\left(1 + \frac{ZY}{2}\right) \tag{2}$$

where β is a propagation constant for Bloch waves and d is the periodicity of the structure. Then, the resonant modes of D-CRLH TL can also be obtained by following condition [13],

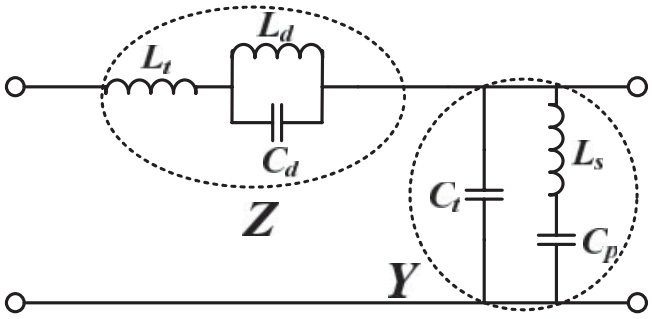

Figure 2 Equivalent circuit of the unit cell of the DGS D-CRLH TL

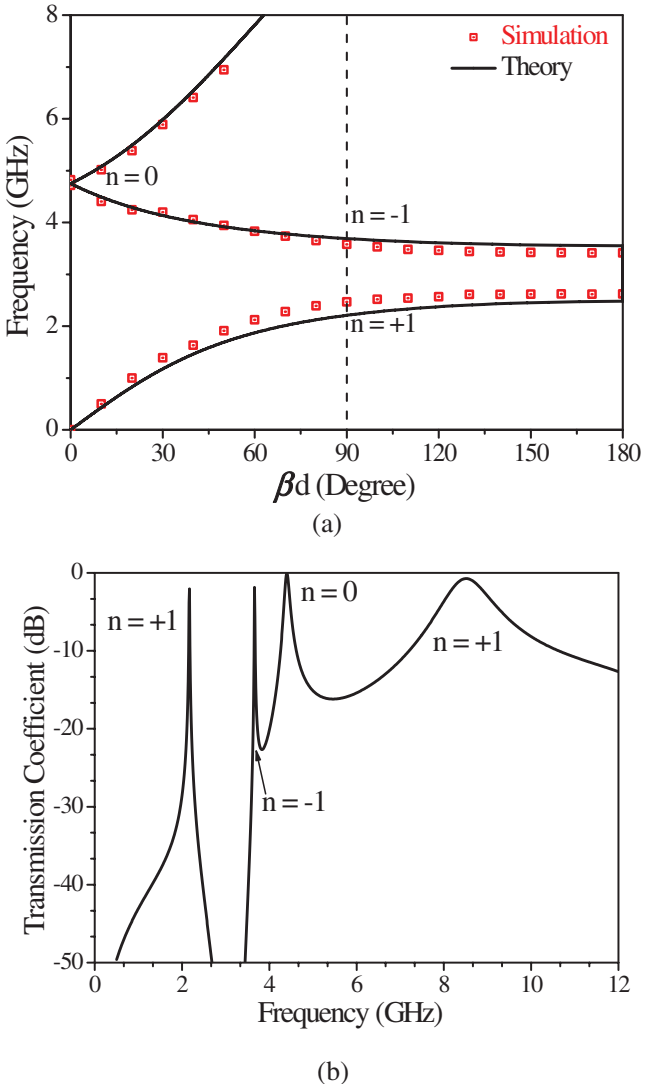

Figure 3 (a) Dispersion curves of the DGS D-CRLH TL (b) Resonant modes of the 2-stage DGS D- CRLH TL resonator. [Color figure can be viewed in the online issue, which is available at www.interscience.wiley.com]

$$\beta_n d = \frac{n\pi d}{l} = \frac{n\pi}{N} \tag{3}$$

$$\begin{cases} n = +1, +2, \cdots, +(N-1) \text{ in the first RH band} \\ \quad = -1, -2, \cdots, -(N-1) \text{ in the LH band} \\ \quad = 0 \text{ at the bondary} \\ \quad = +1, +2, \cdots, +(N-1) \text{ in the second RH band} \end{cases}$$

where N ($= l/d$) and l are the number of unit cell and total length of resonator, respectively.

2.3. Simulation Results for Resonant Modes

Figure 3(a) shows the dispersion curves and the resonant modes of D-CRLH TL using (2) and (3) and full wave simulation. Using a circuit simulator (Ansoft's Designer), the resonant modes of the 2-stage DGS D-CRLH TL resonator having the values of the circuit parameters discussed in the previous section are obtained, as shown in Figure 3(b). It is known that the dispersion curve of D-CRLH TL has three branches within half periodicity (18.1 GHz). Since the TL consists of two unit cells ($N = 2$), the resonator generates two positive, one negative, and zero resonant modes, as

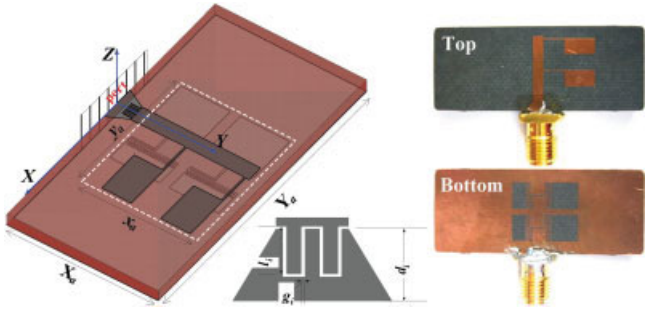

Figure 4 (a) Designed and (b) fabricated triple-band antennas using the 2-stage D-CRLH TL resonator (Rogers RT/Duroid5880 substrate: $h = 1.57$ mm, $\varepsilon_r = 2.2$). [Color figure can be viewed in the online issue, which is available at www.interscience.wiley.com]

shown in (3). These results are confirmed in Figure 3. The resonant frequencies of +1, −1, 0, and +1 mode in Figure 3(b) occur at 2.19, 3.67, 4.39, and 8.56 GHz, respectively. Thus, the multiband antenna can be designed using these resonant modes.

3. MULTIBAND ANTENNA

3.1. Implementation

According to (3), to design a triple band antenna, the D-CRLH TL should have at least two unit cells because three resonance modes are required. The triple band antenna is designed using two cell D-CRLH TL [$N = 2$ in (3)]. Figure 4 shows the designed and fabricated triple band antennas. The feed line for impedance matching between 50Ω port and the antenna is designed by a tapered line with interdigital gap. The length of tapered line (d_i) and interdigital gap (l_i) and gap width (g_i) are set to be 2 mm, 1 mm and 0.05 mm, respectively.

3.2. Full Wave Simulation and Measurement

Figure 5 shows the simulated and measured return losses of the antenna using two cell D-CRLH TL. The resonance frequencies of +1, −1, and 0 mode are measured (simulated) to be 2.57 (2.47) GHz, 3.72 (3.57) GHz, and 4.64 (4.62) GHz, respectively. These measured and simulated results show good agreement with theoretical results from the dispersion curves in Figure 3. It is observed that theoretically unexpected resonant mode is generated in the stop band between +1

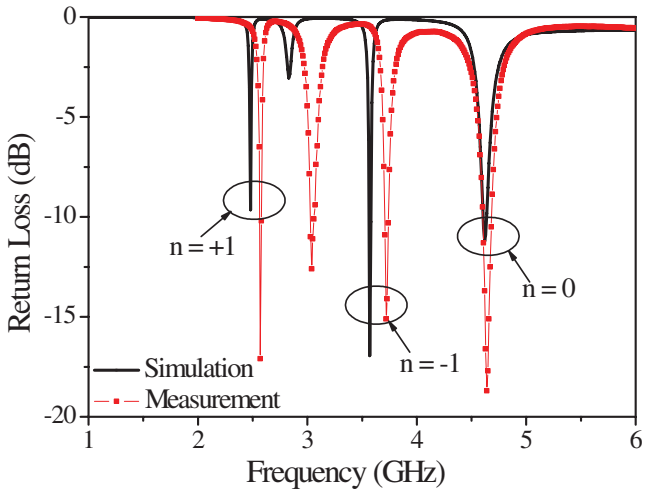

Figure 5 Return loss. [Color figure can be viewed in the online issue, which is available at www.interscience.wiley.com]

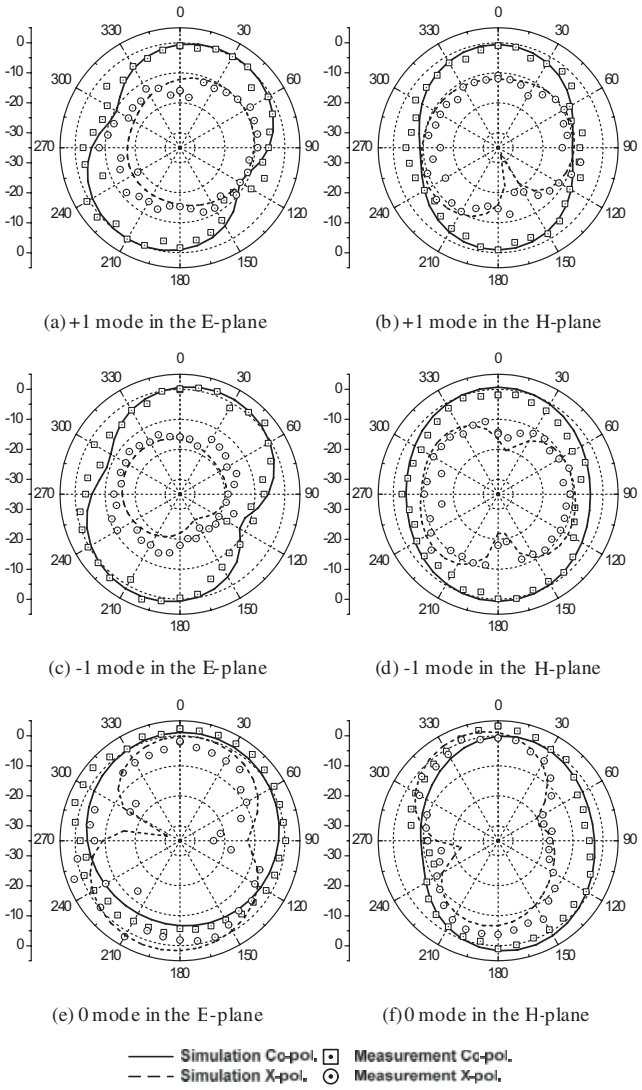

Figure 6 Radiation patterns [phi = 90° → *y*-*z* plane (*E*-plane) and phi = 0° → *x*-*z* plane (*H*-plane)]

mode and −1 mode, as shown in Figure 5. The simulated and measured resonance frequencies of the unexpected mode occur at 2.82 GHz and 3.03 GHz, respectively. It is proven that this resonant mode is excited by the DGS which has radiation loss. In general, the value of the radiation resistance (R) of a typical DGS unit cell is in the range of 600–1500[Ω] at the resonance frequency [14]. Then, this resistance value of R is connected in parallel to L_d and C_d of the equivalent circuit in Figure 2. If the resonance were generated by the DGS without radiation loss, the equivalent circuit in Figure 2 would be open circuit in part of the resonant circuit of DGS. Then, the real part of the input impedance value is to be infinite. Thus, the antenna cannot be matched, so that it cannot radiate. Since the DGS has radiation loss in reality, however, the equivalent circuit is no longer open at the resonance. As the real part of the input impedance value is not infinite, the antenna can radiate if the matching condition is satisfied. This DGS resonance would be helpful and utilized for multiband antenna.

Figure 6 shows the simulated and measured radiation patterns of the antenna at each resonant mode. The measured result agrees with the simulated one, as shown in Figure 6. The maximum gains of the triple band antenna in the *E*-plane (*y*-*z* plane) are measured (simulated) as 0.43 (1.02) dBi, 1.42 (2.26) dBi, and 1.37 (2.82) dBi

TABLE 1 Characteristics of Triple Band Antenna

Mode	Resonance Frequency (GHz) (Sim.,Mea.)	Maximum Gain (dBi) (Sim.,Mea.)	Efficiency (%) (Sim.,Mea.)	Fractional Bandwidth (%) (Sim.,Mea.)	Antenna Size $x_a\lambda_0 \times y_a\lambda_0$ ($X_a\lambda_0 \times Y_a\lambda_0$) (Including Ground)
n = +1	(2.47, 2.57)	*E*-plane : (0.43, 1.02) *H*-plane: (−0.56, −0.97)	(67, 65)	(1.2, 1.7)	$0.096\lambda_0 \times 0.100\lambda_0$ ($0.13\lambda_0 \times 0.32\lambda_0$)
n = −1	(3.57, 3.72)	*E*-plane: (1.42, 2.26) *H*-plane (0.69, 0.34)	(65, 63)	(1.4, 3.2)	$0.138\lambda_0 \times 0.143\lambda_0$ ($0.19\lambda_0 \times 0.47\lambda_0$)
n = 0	(4.62, 4.64)	*E*-plane: (1.37, 2.82) *H*-plane: (1.99, 3.22)	(84, 74)	(4.3, 5.3)	$0.182\lambda_0 \times 0.188\lambda_0$ ($0.24\lambda_0 \times 0.61\lambda_0$)

Sim., simulation; Mea, measurement.

at +1, −1, and 0 mode, respectively. The maximum gains in the *H*-plane (*x*-*z* plane) are also measured (simulated) to be −0.56(−0.97) dBi, 0.69 (0.34) dBi, and 1.99 (3.22) dBi at +1, −1, and 0 mode, respectively. The gain differences between the co- and cross polarization are about 8 dB and 17 dB at +1 and −1 mode in the *E*-plane, respectively. The gain differences are also about 7 dB and 6 dB at +1 and −1mode in the *H*-plane, respectively. The polarization of the antenna at 0 resonant mode is observed to be a right handed circularly polarized (RHCP) due to the circled current flow on the DGS in ground and the rectangular patch in signal line. It is noted that the radiation patterns for each mode are totally tilted with respect to given coordinator due to the asymmetric structure of the antenna.

Table 1 summarizes the characteristics of the multi band antenna such as resonance frequencies, maximum gains, efficiencies, bandwidths and antenna sizes at each mode. The antenna efficiencies are measured by Wheeler cap method [15]. The size of Wheeler cap is 4 cm × 1.6 cm × 1 cm. The dominant resonance frequency of the cavity is 15.46 GHz. Thus, the resonances of antenna are not affected by the resonance of the cavity. In this method, for the accuracy of measurement, there are two important considerations such as good electrical contact between the cap and the ground plane and centering the cap over the antenna [15]. Thus, the difference of efficiency between the simulation and measurement, especially at the zeroth resonant mode, may occur due to the asymmetric structure of the antenna and defected ground plane. Even if the antenna is placed at the center position of the cap, the stub with rectangular patch which determines the zeroth resonant mode [12] cannot be located at the center of the cap due to asymmetric structure. Nevertheless, the measured results of efficiency are quite reasonable.

It is also noted that the differences of bandwidth between the simulation and measurement are caused by the effects of connector and fabrication errors of the dimensional tolerance. Since the connector cable is too close to the antenna, as shown in Figure 4, the connector itself operates as a radiator and, thus, it broadens the measured bandwidth. It is shown that the size of antenna is compact in comparison with conventional patch antenna even if the size of the ground plane is included, as shown in Table 1. Thus, the presented antenna which has the reasonable values of the efficiency, bandwidth, and size are shown to be suitable for multi band antenna as a perfectly planar type.

4. CONCLUSIONS

A multi band antenna using the DGS D-CRLH TL which consists of DGS and stub with rectangular patch has been proposed. The resonant characteristics of the D-CRLH TL resonator are analyzed by theoretical and simulated dispersion curves of the TL. Based on these analyses, the multi band antenna is designed and implemented using 2-stage DGS DCRLH TL resonator. The radiation properties of the antenna such as gains, efficiencies, and bandwidths, are simulated, measured and compared at each mode, respectively. The results show that the proposed antenna can be used as a compact multi band antenna.

ACKNOWLEDGMENT

This work was supported by grant No. 2007-KRF-314-D00188 from the Korea Research Foundation.

REFERENCES

1. D.-U. Sim and J.-I. Choi, A compact wideband modified planar inverted F antenna (PIFA) for 2.4/5-GHz WLAN applications, IEEE Antennas Wireless Propag Lett 5 (2006), 391–394.
2. C.-K. Ham, J.-W. Baik, and Y.-S. Kim, CPW-fed compact meander and L-shape monopole antenna for dual-band WLAN applications, Microwave Opt Technol Lett 50 (2008), 3147–3149.
3. Y.-X. Guo, M.Y.W. Chia, and Z.N. Chen, Miniature built-in multiband antennas for mobile handsets, IEEE Trans Antennas Propag 52 (2004), 1936–1944.
4. C.-Y.-D. Sim, Multiband planar antenna design for mobile handset, Microwave Opt Technol Lett 50 (2008), 1543–1545.
5. J. Romeu and J. Soler, Generalized sierpinski fractal multiband antenna, IEEE Trans Antennas Propag 49 (2001), 1237–1239.
6. H. Li, S. Khan, J. Liu, and S. He, Parametric analysis of sierpinski-like fractal patch antenna for compact and dual band WLAN applications, Microwave Opt Technol Lett 51 (2009), 36–40.
7. A. Lai, K.M.K.H. Leong, and T. Itoh, Metamaterial antennas for dual-band and dual-mode applications, In: Proceedings of the European Conference on Antennas and Propagation (EuCAP), France, 2006.
8. C. Caloz, T. Itoh, and A. Rennings, CRLH metamaterial leaky-wave and resonant antennas, IEEE Antennas Propag Mag 50 (2008), 25–39.
9. C. Caloz, S. Abielmona, H.V. Nguyen, and A. Rennings, Dual composite right/left-handed (D-CRLH) leaky-wave antenna with low beams squinting and tunable group velocity, Phys Status Solidi B 224 (2007), 1219–1226.
10. A. Rennings, T. Liebig, C. Caloz, and I. Wolff, Double-Lorentz transmission line metamaterial and its application to Tri-band devices, IEEE/MTT-S Int Microwave Symp, Honolulu, HI (2007), 1427–1430.
11. Y.H. Ryu, J.H. Park, J.H. Lee, J.Y. Kim, and H.S. Tae, DGS dual composite right/left handed transmission line, IEEE Microwave Wireless Compon Lett 18 (2008) 434–436.
12. Y.H. Ryu, J.H. Park, S.T. Ko, J.H. Lee, and H.S. Tae, Multi-band antenna using dual composite right/left handed transmission line, IEEE Antennas Propag Int Symp, San Diego, CA (2008).
13. C. Caloz and T. Itoh, Electromagnetic metamaterials: Transmission line theory and microwave applications, Wiley, New York, 2006.
14. H. Kim and B. Lee, Bandgap and slow/fast-wave characteristics of defected ground structures (DGSs) including left-handed features, IEEE Trans Microwave Theory Tech 54 (2006), 3113–3120.
15. D. M. Pozar and B. Kaufaman, Comparison of three methods for the measurement of printed antenna efficiency, IEEE Trans Antennas Propag 36 (1988) 136–139.